**Analele Universităţii de Vest din Timişoara**
**Vol. XLVIII, 2006**
**Seria Fizică**

# ADVANCED MAGNETIC MATERIALS FOR TECHNICAL APPLICATIONS

E. Burzo

*Faculty of Physics, Babes-Bolyai University, 400084 Cluj-Napoca, Romania*

**Abstract**
The evolution and the main properties of hard and soft magnetic materials is firstly presented. Then, we analyse the magnetic characteristic of nanocrystalline systems based on Nd-Fe-B, Sm-Fe-Si, Zr-Co-Fe and FeSiBNbCu. Representative magnetostrictive and magnetocaloric materials are described. Finally, we analyse the physical properties of Sr2FeMoO6 perovskite.

## 1. Introduction

The elaboration of magnetic materials having technical applications started in the first part of 20 century and since then, researches for improving their performances have shown continuous growth. New hard, semi-hard and soft magnetic materials were developed. The relative weight of magnetic materials, manufactured in the recent years are plotted in Fig. 1. High performances materials, recently elaborated, grow continuously as importance, particularly those involved in information technology.

The evolution of the coercive field values for hard and soft magnetic materials, during last 100 years, is shown in Fig. 2. Hard magnetic materials with coercivities higher than 107 A/m were obtained. Soft magnetic materials are now discovered, having coercivities of the order of 10-1 A/m.

The elaboration of high energy permanent magnets started in 1967 year, when SmCo5-type magnets were obtained and continued to discovery in 1984 of Nd-Fe-B magnets. Although the Nd-Fe-B magnets have very high energy product, the Curie points are rather low. Studies were performed to improve their performances at higher temperatures, as well as to obtain new types of permanent magnets based on rare-earth-iron or magnets without rare-earths. In this context, in the following, we analyse the magnetic properties of new types of permanent magnets as Sm-Fe-Si or Zr-Co-Fe and some nanocomposite systems. The nanomaterials having very low

coercivities are also presented. Some results obtained by the study of magnetoresistive, magnetocaloric and magnetostrictive materials are also given.

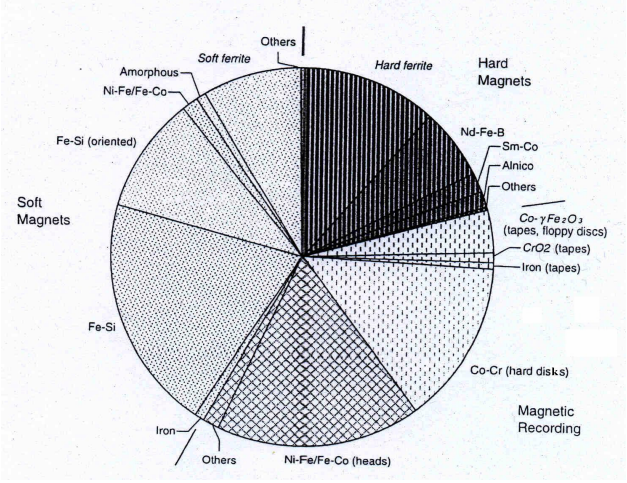


*Fig.1 The actual production of magnetic materials at the world scale.*

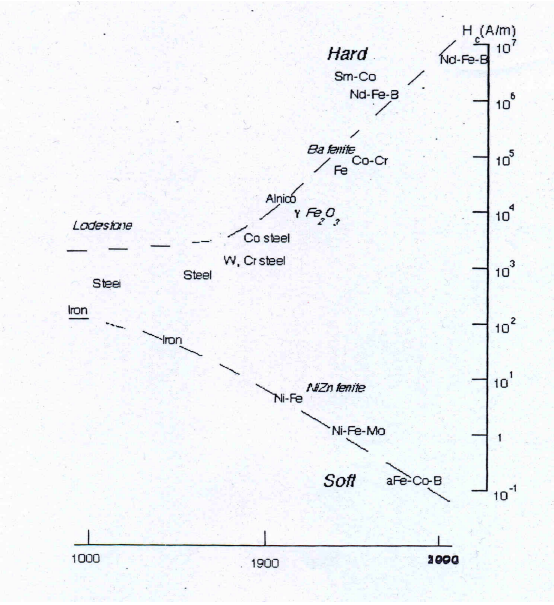


*Fig.2 The evolution in time of the coercive fields for hard and soft magnetic materials.*

## 2. Hard Magnetic Materials

The evolution of the maximum energy product in last 100 years showed an exponential increase described by the relation $(BH)max = 9.6 \exp[(year - 1910)/\delta]$ with $\delta = 20$ years. Thus, the (BH)max values increased by $e = 2.7$, every 20 years. The remarkable evolution was determined by the discovery of intermetallic compounds based on transition metal-rare-earth, particularly light ones. In this case the magnetic moments are parallely aligned ensuring a high saturation induction. The magnets are relatively expensive since of the presence of rare-earths. The terrestrial abundance of rare-earths is given in Fig. 3. The most abundant are Pr and Nd, while Sm are little in terrestrial area and consequently expensive.

The SmCo5 and Sm2Co17-based permanent magnets have a good thermal stability since of their high Curie temperatures ($Tc > 1000$ K) [1]. Both Sm and Co are very expensive. Consequently the researches have been directed for development of cheaper permanent magnets, particularly based on iron [2]. In 1984 were discovered the Nd-Fe-B magnets, having high energy product [3]. The hard magnetic properties are given by the Nd2Fe14B phase. The compound crystallizes in a tetragonal structure – Fig. 4. This phase has a low Curie temperature, $Tc \cong 580$ K. Although 90 % of atoms are magnetic, the Tc value is about half that of iron. Consequently,

these magnets can be used only in limited temperature range above room temperature. The above bahaviour can be correlated with the complex crystal structure of hard magnetic phase in which iron occupies 6 types of sites, Nd two and B one. The distances between iron atoms cover a large range of values. For distances between iron atoms smaller than ≅ 2.50 Å, the exchange interactions are negative, while for higher distances these are positive – Fig. 5. Since the positive interactions are dominant, the negative ones are not satisfied and consequently a considerable magnetic energy is stored. As a consequence, there is a high decrease of the Curie temperature. We analysed the possibility for increasing Curie temperature by substituting iron atoms involved in negative exchange interactions [2,4]. Some results are given Fig. 6. The most benefic effect on Tc values is given by cobalt. Cobalt decreases the anisotropy and coercive field, respectively, while Al increase de coercive field but decrease Curie temperature. Consequently, the effect of both Co+Al substitutions was analysed [5]. A good compromise between an increased Curie temperature and coercive field was finally obtained. The substitutions of iron by nonmagnetic elements such as Cu, Si or Ga increase also Tc values. These atoms replace part of iron involved in negative exchange interactions and their contributions to exchange interactions are diminished.

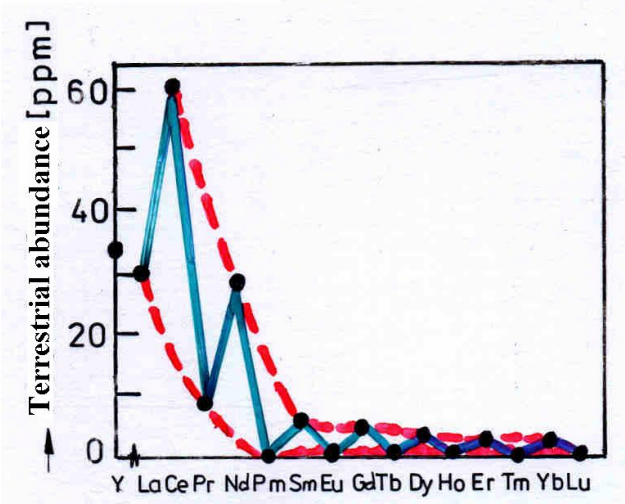


*Fig.3 Terrestrial abundance of the rare earths*

Another way to obtain permanent magnets based on Nd-Fe-B is to produce nanocomposite systems [6]. These are formed from two magnetic phases, one hard as Nd2Fe14B and another soft as α-Fe of Fe3B. Referring to the boron content, in the original alloy, two types of nanostructures were obtained. As example, in Nd15Fe77B18.8 this is formed from Nd2Fe14B + Fe3B + α - Fe. The alloys with low boron content, as Nd6Fe88B6, are constituted from Nd2Fe14B + α-Fe. The Nd5Fe66.5Cr10MxB18.5 with M = V, Nb were obtained by melt spinning. The thermal, treatment, at 6500C, leads to crystallization of the alloys [7]. Unlike other

systems having high boron content, for a short annealing time, the presence of α-Fe was found. The mean dimensions of α-Fe crystallites increase rapidly for an annealing time up to ta = 1 min, at 6500C and then a nearly linear variation was observed – Fig. 7. For ta = 10 min, the mean grain size of α-Fe is d=17 nm. Due to the small crystallite dimensions, the as quenched samples are superparamagnetic. The hard magnetic phase was developed after crystallization of as-,quenched samples. Both the remanent induction and the coercive field increase gradually with annealing time–Fig.8. For samples thermally treated at 6500C, during 10 min a ratio of remanent to saturation induction, Br/Bs = 0.7, was determined. The high value of the remanence ratio is due to the exchange coupling between the magnetic moments at the interface of the hard and soft magnetic nanograins. As a consequence of this coupling, there is a large degree of reversibility in the demagnetization behaviour. The exchange interactions would suppress the reversible rotation of the magnetization in the soft α-Fe particles and there is a significant increase of the coercivity.

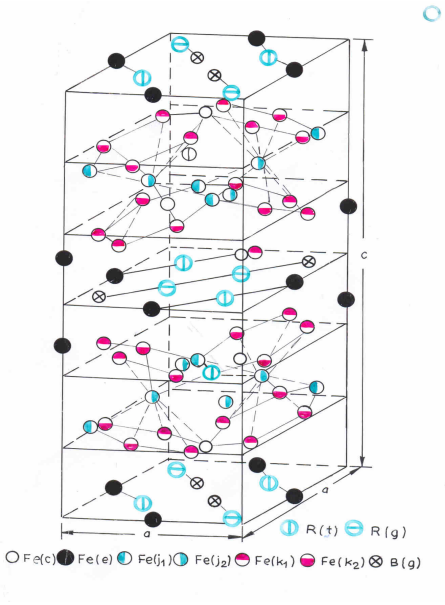


*Fig.4 Crystal structure of the $Nd_2Fe_{14}B$ hard magnetic phase*

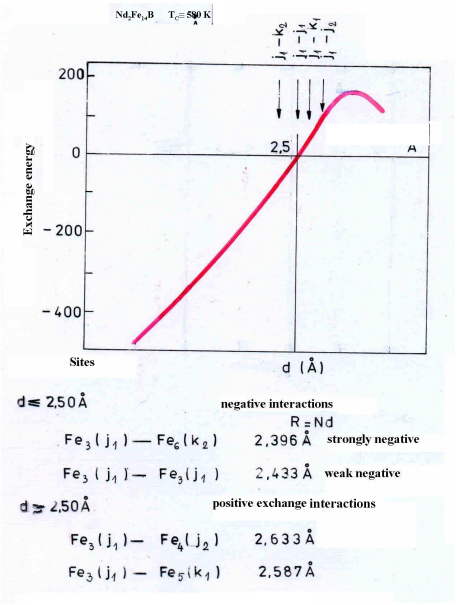


*Fig.5 The Néel-Stater curve and the distances between iron atoms in $Nd_2Fe_{14}B$ compound*

We analysed the possibility to have alloys with high coercivities in R-Fe-Si system [8,9]. In the R-Fe phase diagram, unlike R-Co one, the 1/5 type compounds were not found. The compounds with highest iron content are of R2Fe17-type. These compounds have a very low Curie temperatures (< 450 K) although the iron moments are close to that of pure iron. The

anisotropy is planar and thus cannot be used as starting materials for obtaining permanent magnets. The researches were directed to metastable phases of Sm-Fe alloys having compositions R/Fe between 1/5 and 1/9. The compositions in the studied region can be described by R1-sFe5+2s. For s = 0.22, a TbCu7 type structure can be invoked, while for s = 0.36–0.38, a 1/9 stoichiometry was found. If s = 0.33, a single R atom of three was substituted for by one dumbbell pair and the stoichiometry was 2/17. If the dumbbell pairs are randomly distributed, the structure is closely related to 1/5 type.

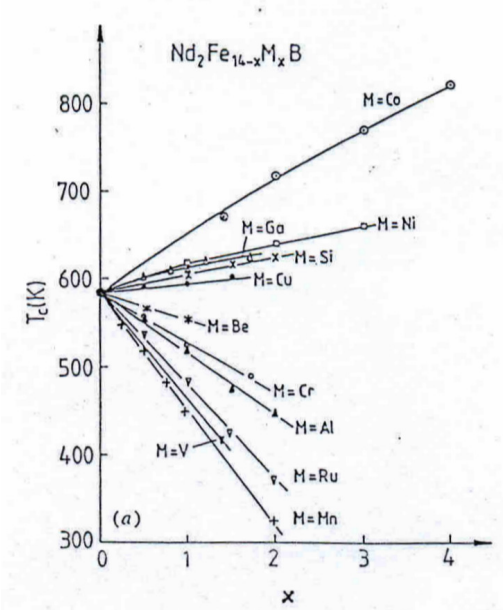


*Fig.6 The effect of iron substitutions by various elements (M) on the Curie temperatures of $Nd_2Fe_{14-x}M_xB$ compounds.*

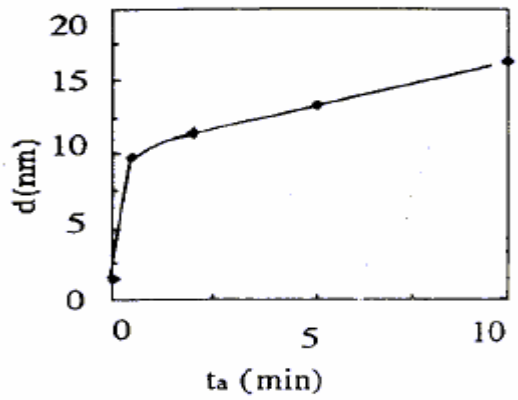


*Fig.7 The α-Fe crystallite sizes as a function of the annealing time at 650 $^oC$ for $Nd_5Fe_{66.5}Cr_{10}Nb_2B_{18.5}$ nanocrystalline alloy.*

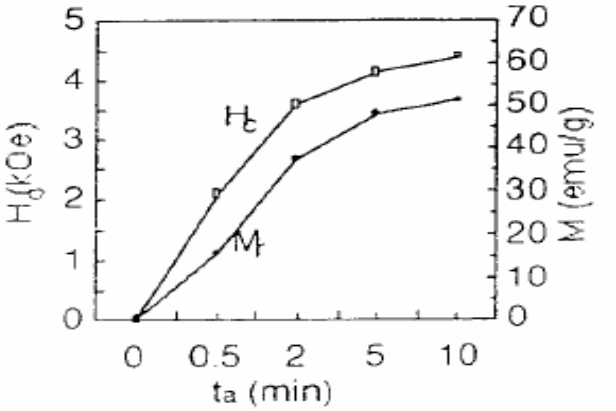


*Fig.8 Remanences and coercivities for $Nd_5Fe_{66.5}Cr_{10}Nb_2B_{18.5}$ nanocrystalline alloy.*

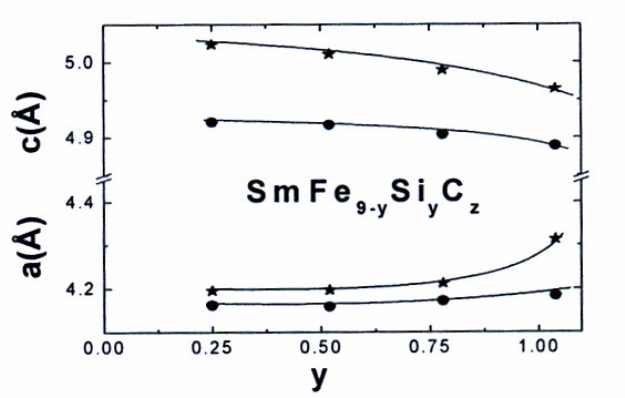


*Fig.9 Lattice parameters of $SmFe_{9-y}Si_yC_z$ (z = 0,1) nanocrystalline alloys.*

The SmFe9-ySiy nanocrystalline alloys were prepared by high energy ball milling. A P6/mmm type structure was obtained after annealing at 650-8500C. In order to avoid the presence of negative exchange interactions, in addition to silicon substitution, the samples were carbonated. The composition dependences of the lattice parameters are given in Fig.9. The increase of lattice parameters of carbonated samples leads to an increase of distances between iron atoms above the value of 2.50 Å and consequently the Curie temperatures will increase – Fig. 10. The Tc value, for a composition y = 0.5, is 670 K. In addition, the anisotropy changed from planar to uniaxial. The coercivities of carbonated samples as function of annealing temperatures and compositions are plotted in Fig.11. A coercive field of μ0Hc = 1.3 T was found in case of the sample having y=0.50 and grain sizes around 22 nm. The highest coercive field, μ0Hc = 1.5 T, was obtained for a SmFe8.75Si0.25C alloy. These alloys have good potential for technical applications. The high coercivities of mechanically alloyed and carbonated samples, originate from the presence of the 1/9 metastable phase.

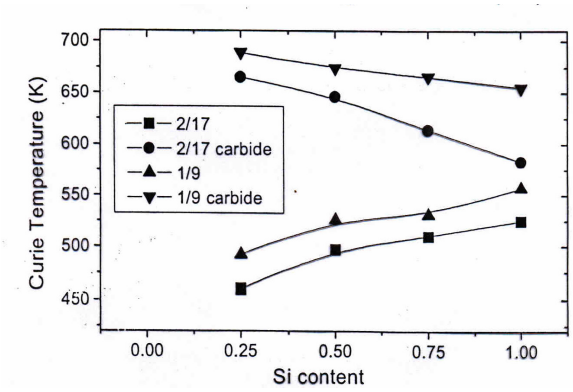


*Fig.10 The Curie temperatures of $SmFe_{9-y}Si_yC_z$ and $SmFe_{8.5-y}Si_yC_z$ (z = 0, 1) nanocrystalline alloys*

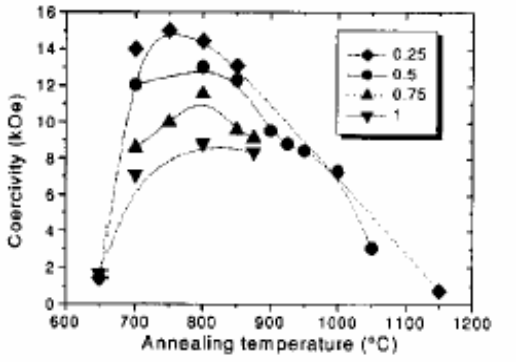


*Fig.11 Coercive fields as function of annealing temperatures and compositions for $SmFe_{9-y}Si_yC$ nanocrystalline alloys.*

We analysed the possibility to have hard magnetic properties in alloys without rare-earth. For this reason we preparated the ZrCo5.1-xFex compounds both as bulk and in nanocrystalline state [10,11]. The ZrCo5.1 crystallizes in a rhombohedral and orthorhombic type structures, corresponding to high- and low-temperature phases. The composition dependences of the Curie temperatures and saturation magnetizations, at 4.2 K, for both microcrystalline and nanocrystalline systems are plotted in Fig.12. There is an increase of both Tc and Ms values when cobalt is substituted by iron. The saturation magnetizations of nanocrystalline systems are higher than of bulk materials. This behaviour can be related to a more random distribution of substituting atoms in lattice. The temperature and composition dependences of the anisotropy fields are shown in Fig.13. The anisotropy field, at 300 K, in ZrCo5.1 is μ0Hc = 3.5 T. This decrease rapidly when the cobalt is partially replaced by iron. The anisotropy field, for iron-doped compounds increases up to T ≅ 300 K and then decreases. This unusual behaviour might be explained assuming anisotropy contributions of different signs, for different transition metal sites. Since of high anisotropy field, this system shows good hard magnetic properties.

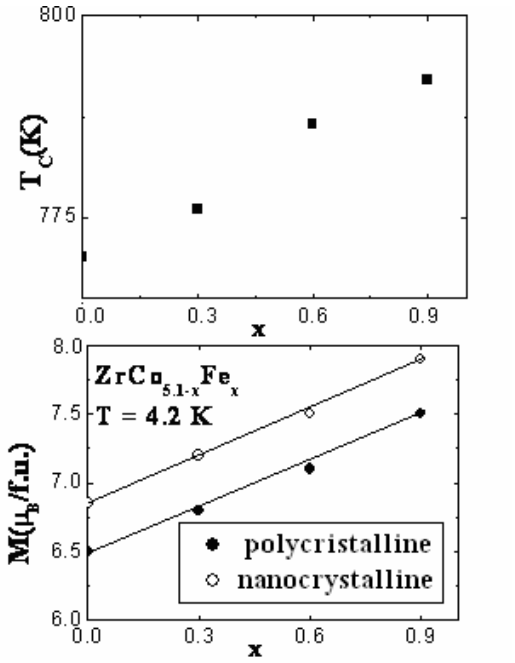


*Fig.12 Composition dependence of the saturation magnetizations at 4.2 K for $ZrCo_{5.1-x}Fe_x$ bulk and nanocrystalline alloys as well as of the Curie temperatures.*

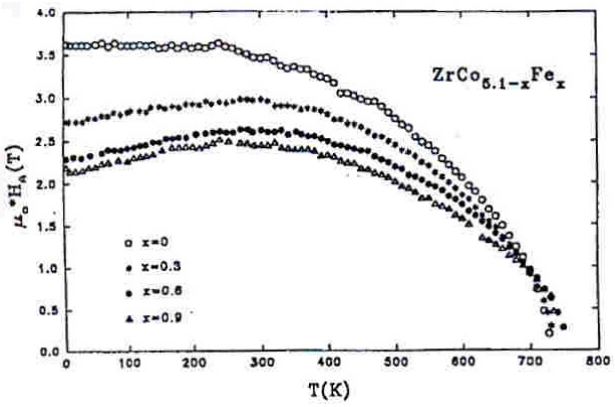


*Fig.13 Thermal variations of the anisotropy fields in $ZrCo_{5.1-x}Fe_x$ alloys.*

### 3. Nanocrystalline soft magnetic materials

The iron based nanocrystalline alloys constitute a new class of ultrasoft magnetic materials. The high permeability, good thermal stability and small losses make these materials of interest for technical applications. The particularity of these materials is their fine structure consisting of bcc FeSi grains distributed in an amorphous matrix. The Fe-Si-B-Nb-Cu alloys were obtained by splat cooling, as amorphous, followed by a recrystallization thermal treatment, at 470-550 oC. The nanocrystalline structure is essentially connected with the presence of Cu and Nb and their small solubility in bcc FeSi grains [12]. After the crystallization process was thermally activated, the copper atoms tend to be concentrated as clusters of nanometer sizes. The iron atoms are expelled from such copper zones. The regions having high iron concentrations constitute the nucleation sites for α-FeSi grains. The increase of the grains dimensions is limited by the presence of Nb atoms, expelled from grains and located in the amorphous phase. Boron is used to facilitate the formation of amorphous phase. Finally, there are bcc FeSi grains having d ≤ 15 nm dimensions, homogeneous distributed in the material volume and separated by a FeNbBCu matrix. The maximum crystalline fraction of alloy is 80 %. The quasistatic hysteresis cycle for a composition Fe73.5Si13.5B9Nb3Cu1 is given in Fig.14 [13]. There is a very narrow hysteresis cycle. The coercive field is of the order of 0.7 A/m, situated at the end of curve describing the variation of the coercive field in soft magnetic materials, as showed in Fig.2.

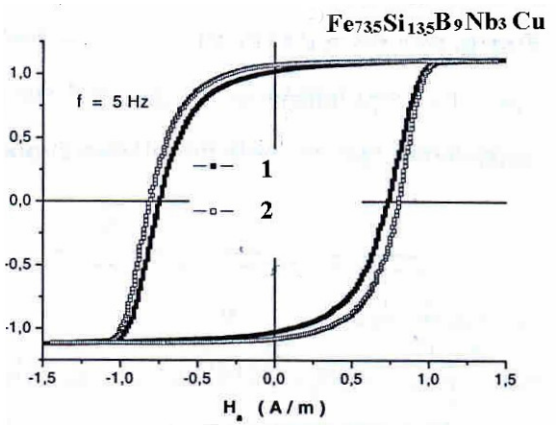


*Fig.14 Hysteresis cycles of two nanocrystalline $Fe_{73.5}Si_{13.5}B_9Nb_3Cu$ samples.*

### 4. Magnetostrictive compounds

The non-S state heavy rare-earth (R) have, at low temperatures, high magnetostriction, λ. The λ values obtained at 4.2 K are ≅ 9·10-3 for Tb and Dy and 2.5·10-3 for Ho. Since of low Curie temperatures of the above metals, these cannot be used in devices working at room

temperature. In the Laves phase compounds, RFe2, on the support of R-Fe exchange interactions, the Curie temperatures increased up to 697 K (TbFe2), 635 K (DyFe2) and 597 K (HoFe2). Thus, the large magnetostricition (characteristic to R metals at low temperatures) can be translated at higher temperatures. In Fig.15 we present the thermal variation of spontaneous magnetizations and of reciprocal susceptibilities for TbFe2, DyFe2 and HoFe2 [1,14]. The magnetostricitions of the RFe2 compounds, at room temperature, are shown in Fig.16 [15]. The SmFe2, TbFe2 and DyFe2 exhibit the highest room temperature magnetostriction, but relatively large magnetic field are needed for achieving the technical saturation, due to the very large magnetocrystalline anisotropy energy. Considering that both the magnetostriction and the magnetocrystalline anisotropy present a single-ion character, two different compounds, exhibiting anisotropy coefficients of different sign were alloyed. Thus, was obtained a ternary alloy, as Tb0.3Dy0.7Fe2, with still large magnetostricition at room temperature (1.5·10-3), but a magnetocrystalline anisotropy energy strongly reduced [15]. This opened the era for technical applications of the large magnetostrictive systems based on rare earth metals.

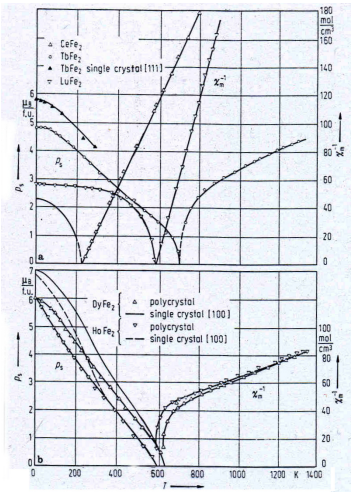


*Fig.15 Thermal variations of spontaneous magnetizations and of reciprocal susceptibilities for $CeFe_2$, $TbFe_2$, $DyFe_2$ and $HoFe_2$. The data obtained on single crystals are also plotted.*

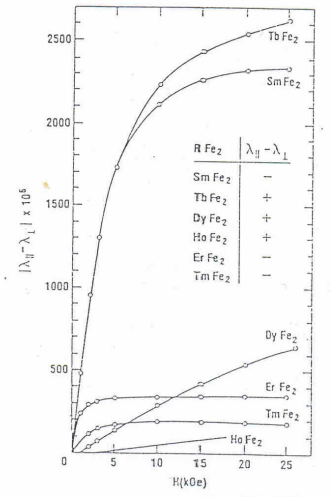


*Fig.16 Field dependence of the manetostriction in $RFe_2$ compounds*

### 5. Magnetocaloric materials

Recently, interest in research into magnetocaloric effect (MCE) has been considerably enhanced due to its potential impact on energy savings and environmental benefits. The magnetic

refrigerators are based on the magnetocaloric effect, i.e. the magnetic entropy change induced by the changes in the external magnetic field applied to the magnetic materials. Under adiabatic conditions, the change in magnetic entropy is compensated by an equal and inverse change in lattice entropy which causes a variation in the temperature of the material. A variety of prototype materials and intermetallic compounds was studied in order to achieve a large MCE, at requested temperature. This can involve MCE effect, at room temperature, or at smaller ones particularly for liquefaction of nitrogen, hydrogen or helium. The large MCE can be obtained for materials having large magnetic moment and also a sharp drop of the magnetization with increasing temperature, associated with the magnetic phase transition [16].

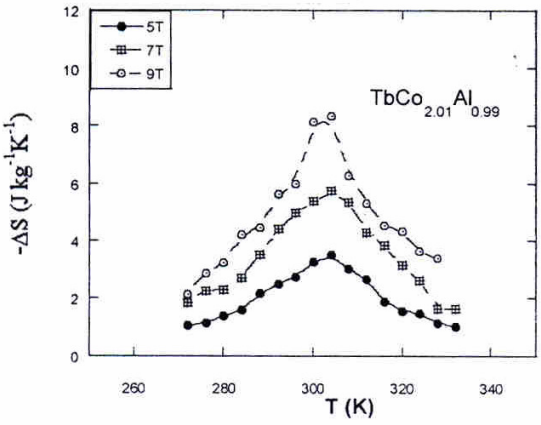


*Fig.17 Magnetic entropy changes in $TbCo_{2.01}Al_{0.99}$ compound.*

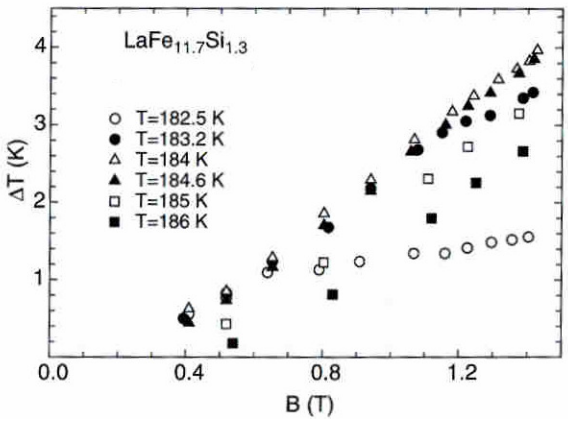


*Fig.18 Adiabatic temperature change of $LaFe_{11.7}Si_{1.3}$ as function of the field.*

Rare earth intermetallic compounds are promising candidates for magnetic refrigeration applications because of their large magnetocaloric effect in the vicinity of the magnetic phase transition. Thus, we studied the magnetocaloric effects in some systems. As example we present in Fig.17 the entropy changes in TbCo2.01Al0.99 [17]. A value $-\Delta S \cong 9$ JkgK-1 was obtained around room temperatures, in field of μoH=9 T. The adiabatic temperature change in LaFe11.7Si1.3 is shown in Fig.18 [18]. A linear dependence of $\Delta T = |Tc-T|$ on the applied field was observed above 183.2 K. The maximum value, of 4 K, was obtained for $\Delta T = 2.4$ K. The appreciably large values of the MCE were attributed to release of the entropy due to first-order phase transition induced by external magnetic field.

**6. Magnetoresisitve Sr2FeMoO6 compounds**

The Fe and Mo atoms, in the perfectly crystalline structure of Sr2FeMoO6, are alternatively arranged along the axes of tetragonal structure and separated by oxygen atoms. In a real structure there are antisite defects; a fraction of Mo ions can occupy Fe sublattice sites and conversely. The XPS studies of the Mo3d and Fe3s core levels is indicating the existence of both Fe3+-Mo5+ and Fe2+-Mo6+ states [19]. Two samples were studied having 3 % (sample 1) and 5 % (sample 2) antisite defects. At 4.2 K, the saturation magnetizations, Ms, were 3.5 μB/f.u. (sample 1) and 3.3 μB/f.u. (sample 2). From these data we estimated 6 % and 8 % antisites respectively, not very different from the values obtained from X-ray analyses. The HRTEM studies [20] showed that the microstructure of sample 1 consists from grains having 0.2-0.4 μm diameter and also regions in which the grains coalesced in bands. The presence of grains having 2-3 μm diameter were shown in sample 2. The iron content of sample 1 was somewhat smaller that the ideal value (25 at %), while in case of sample 2 was higher than 25 at % - Table 1.

*Table 1 Mean compositions and 57Fe hyperfine parameters*

| Sample | Composition (%) | | | Sites | | | | | | | | | |
|---|---|---|---|---|---|---|---|---|---|---|---|---|---|
| | | | | M1 | | M1' | | M2 | | AS | | APB | |
| | Sr | Fe | Mo | Bhf (T) | A (%) | Bhf (T) | A (%) | Bhf (T) | A (%) | Bhf (T) | A (%) | Bhf (T) | A (%) |
| Grain (1) | 53.53 | 21.03 | 25.44 | | | | | | | | | | |
| boundary (1) | 52.97 | 21.70 | 25.33 | 45.8 | 71.5 | | | 48.3 | 18.8 | 54 | 5.8 | 8.4 | 3.9 |
| Grain (2) | 51.02 | 26.00 | 22.98 | | | | | | | | | | |
| boundary (2) | 50.19 | 27.57 | 22.24 | 46.9 | 62.5 | 50.7 | 12.2 | 49.4 | 12.6 | 59 | 6.2 | 5.7 | 6.5 |

Negative magnetoresistances (MR) were evidenced for both samples, but having different behaviours as function of temperature and field – Fig.19. At 9K, the MR values for samples 1 was 14 % in field of 1 T and 34 % at 7 T. The magnetoresistances, at the same temperature, are smaller in sample 2, being 7 % in field of 1 T and 17 % at 7 T. At 250 K, the MR values are nearly the same as that at 9 K for sample 1, but for sample 2 is around 6 % in fields higher than μoH = 5 T .

The 57Fe hyperfine parameters are listed in Table 1. The M1 sextet was attributed to iron in mixed valence Fe2+/Fe3+ state, at right sites and the AS one to iron located in antisites. The M2 sextet arises from iron ions adjacent to AS sites and the sextet with the smallest hyperfine field to iron located in antiphase domain boundaries (APB). In case of sample 2, the best fit was obtained considering an additional sextet (M1') attributed to iron in mixed valence state in right

sites, having higher hyperfine field, Bhf, than determined for sextet M1. The presence of two sextets may be correlated with a variable Fe/Mo ratio inside the grains. The above data suggest that differences in the magnetoresistivities of the two samples may be correlated with both the composition and the distribution of ions inside the grains. The nonuniform distribution can be correlated with the grains having larger dimensions. The excess of iron in sample 2 seems to influence strongly the conduction behaviour, in addition to nanosized Fe and/or Mo rich regions located inside the grains. Thus, the resisitivities of Sr2FeMoO6 seem to be determined by many factors including antisite defects, compositions and their nonuniformity inside the grain boundaries.

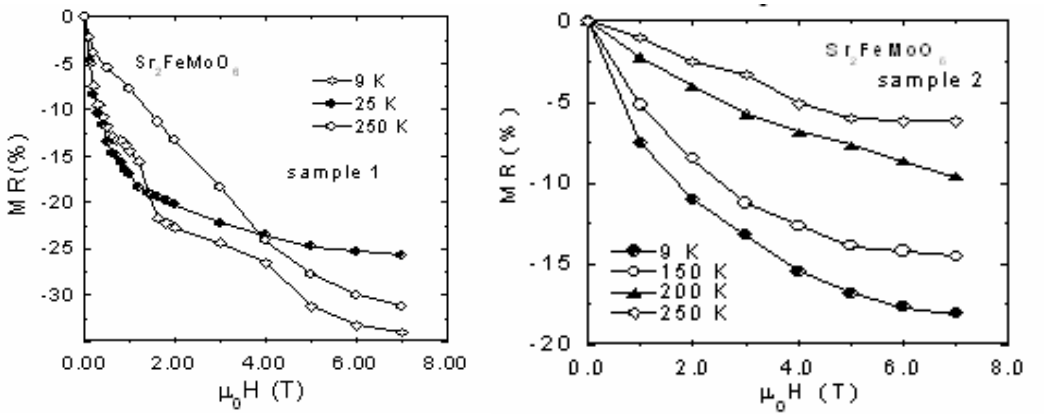


*Fig.19 The field and temperature dependences of the magnetoresistivities for two Sr2FeMoO6 perovskites.*

### 7. Conclusions

In recent years, the researche activities on magnetic materials, particularly nanomaterials are growing. New materials having possible technical applications were studied and applied in economy and social life. These are essentially in the development of society based on knowledge.

### References

[1] E.Burzo, A.Chelkovski and H.RKirchmayr, Landolt Börnstein Handbuch, Springer Verlag, 1990 vol. III/19d2

[2] E.Burzo, Rep. Progr. Physics 61, 1099 (1998)

[3] M.Sagawa, S.Fujimura, M. Tagawa, H. Yamamoto, Y.Matsura, J.Appl. Phys. 55, 2083 (1984)

[4] E.Burzo, E.B. Boltich, M.Q. Huang and W.E. Wallace, Proc. 8th Int. Workshop on Rare-Earth Magnets and Their Applications, Dayton, 1985 p. 711

[5] E.Burzo, L. Stanciu and W.E. Wallace, J.Less Common Met 111, 83 (1985)

[6] A.T. Pedziwiatr, W.E.Wallace and E.Burzo, Solid State Commun. 61, 61 (1987)

[7] E.Burzo, A.T. Pedziawiatr and W.E. Wallace, Solid State Commun. 61, 57 (1987)

[8] R.Coehoorn, B. De Mooji, J.P.W.B. Duchateau, K.H.J. Buchow: J. Phys. 49, C8-669 (1998)

[9] E.Burzo, C.Djega-Mariadassou in Nanoscale Devices-Fundamental and Applications, Springer Verlag, 2006 p. 371-385

[10] C.Djega, L.Bessais, A.Nandra, J.M. Grenche and E.Burzo, Phys. Rev. B65, 014419, 2001

[11] C.Djega, L.Bessais, A.Nandra and E.Burzo, Phys. Rev. B68, 024406 (2003)

[12] E.Burzo et al, J.Appl. Phys. 70, 6550 (1991)

[13] E.Burzo, E.Dorolti and C.Djega, be published

[14] Y.Yoshizawa, S.Ogawa and K.Yamauchi, J.Appl. Phys. 64, 6044 (1988)

[15] L.Fratila, Ph.D. Thesis, University Babes-Bolyai- University J. Fourier, 2002

[16] E.Burzo, Zeit. Angew. Physik 32, 127 (1971)

[17] A.E.Clark, Ferromagnetic Mat., vol. 1, Ed. E.P. Wohlfarth, N. Holand, Amsterdam, 1980

[18] A.M. Tishin: Handbook of Magnetic Materials, Ed. K. H. J. Buschow, Elsevier, 1999 p. 395

[19] R. Tetean, E.Burzo and I.G. Deac, J. Opt. Adv. Mat. 8, 501 (2006)

[20] M.Ilyn, A.M. Tishin, F. X. Yu, J.Gao, J.R. Sun, B. G. Shen, J. Magn. Magn. Mat. 290-291, 712 (2005)

[21] K.Kupper, I.Balasz, H.Hesse, A.Takacs, T.Crainic, K.C.Prince, M.Matteucci, D.Wett, R.Szargan, E.Burzo and M.Neumann, Phys. Stat. Solidi (a) 201, 3252 (2004)

[22] E.Burzo, I.Balasz, S.Constantinescu and I.G.Deac, J.Magn.Magn. Mat. (in press)